

# Variable Step Size Maximum Power Point Tracker Using a Single Variable for Stand-alone Battery Storage PV Systems

Emad M. Ahmed<sup>†</sup> and Masahito Shoyama\*

<sup>†</sup>\* Graduate School of Information Science and Electrical Engineering, Kyushu University, Fukuoka, Japan

## Abstract

The subject of variable step size maximum power point tracking (MPPT) algorithms has been addressed in the literature. However, most of the addressed algorithms tune the variable step size according to two variables: the photovoltaic (PV) array voltage ( $V_{PV}$ ) and the PV array current ( $I_{PV}$ ). Therefore, both the PV array current and voltage have to be measured. Recently, maximum power point trackers that are based on a single variable ( $I_{PV}$  or  $V_{PV}$ ) have received a great deal of attention due to their simplicity and ease of implementation, when compared to other tracking techniques. In this paper, two methods have been proposed to design a variable step size MPPT algorithm using only a single current sensor for stand-alone battery storage PV systems. These methods utilize only the relationship between the PV array measured current and the converter duty cycle ( $D$ ) to automatically adapt the step change in the duty cycle to reach the maximum power point (MPP) of the PV array. Detailed analyses and flowcharts of the proposed methods are included. Moreover, a comparison has been made between the proposed methods to investigate their performance in the transient and steady states. Finally, experimental results with field programmable gate arrays (FPGAs) are presented to verify the performance of the proposed methods.

**Key Words:** Field programmable gate arrays, Fixed step size, Maximum power point (MPP), Maximum power point tracking (MPPT), PV array, Single current sensor, Stand-alone Battery Storage, Variable step size

## I. INTRODUCTION

The growing demand for energy, together with the increase in price for oil products and the attention being paid to environmental pollution, have been progressively increasing the interest in renewable energy sources. Many renewable energy sources are now available; among these, solar energy seems to be the most promising for widespread utilization. Many applications employing this technology have been developed, such as solar power generation, solar vehicle construction, battery charging, water pumping, satellite power systems, and so on [1], [2].

In most photovoltaic applications, maximum power point tracking (MPPT) is an essential issue as there is a probable mismatch between the load characteristics (i.e., constant power, constant voltage, and constant current) and the maximum power points (MPPs) of the PV array [3], [4]. The (P-V) characteristic under different irradiation levels is shown in Fig.1.

The non-linear variation in the output voltage and current, which depend on the solar-radiation level, operating temperature and load current, can cause low electrical efficiency [5],

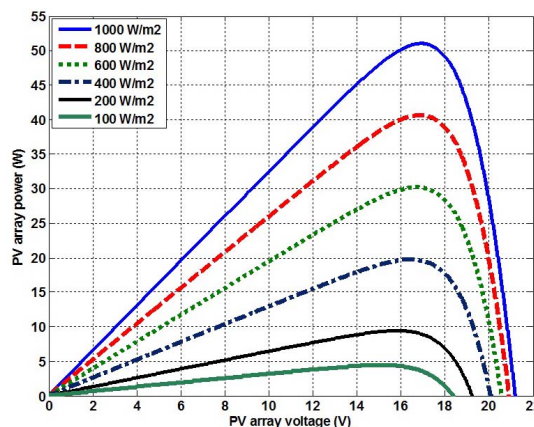


Fig. 1. Power-voltage characteristics of photovoltaic module at different irradiance levels with constant temperature (25°C).

and [6]. To solve these problems in the utilization of solar arrays for electrical power, the MPP of a PV system is tracked using tracking algorithms, where the system operating point is forced towards the optimal operating conditions.

Maximum power point tracking algorithms can be broadly classified as either online or offline. The offline methods do not measure the actual extracted power of the PV panel, which can be used to calculate the required update on the operation of the power converter. They are based on prior knowledge of the photovoltaic panel characteristics and measurements of

Manuscript received Oct. 21, 2010; revised Jan. 29, 2011

<sup>†</sup> Corresponding Author: El-bakoury@ieee.org

Tel: +81-92-802-3704, Fax: +81-92-802-3703, Kyushu University

\* Graduate School of Information Science and Electrical Engineering, Kyushu University, Japan

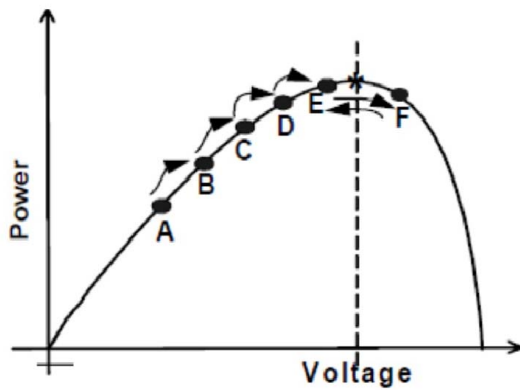


Fig. 2. Conventional fixed step size MPPT operation.

solar irradiation, such as the short circuit current ( $I_{sc}$ ), and the open circuit voltage ( $V_{oc}$ ) [1], [7]. Therefore, these algorithms cannot detect the maximum power point very accurately, especially during rapid variation in atmospheric conditions.

On the other hand, online algorithms such as the perturbation and observation (P&O) algorithm, the hill climbing (HC) algorithm, the incremental conductance method (INC), the ripple correlation control (RCC), and the single variable maximum power point tracker method, are based on the actual measured values of  $V_{PV}$  or  $I_{PV}$  or both to force the system operating point towards the maximum power point [8]–[13]. Therefore, the online algorithms are considered to be true maximum power point trackers.

The P&O algorithm operates by periodically perturbing the control variable and then comparing the instantaneous PV output power after perturbation with the value before perturbation. In an original MPPT controller using the P&O method, the adjustment of the operating point is achieved by changing the reference voltage of the controller. However, the adjustment can also be made through the duty ratio as in the HC algorithm [14].

The P&O and HC methods involve a perturbation in the operating voltage and the converter duty ratio, respectively. Therefore, steady state oscillations always appear in both techniques in the neighborhood of the MPP due to the fixed perturbation as shown in Fig. 2. Thus, the total efficiency of the PV generating systems utilizing these methods will decrease.

On the other hand, the INC method, which is based on the fact that the slope of a PV array power versus the PV array voltage is zero at the MPP, has been proposed to improve the tracking accuracy and the dynamic performance under rapidly varying conditions [15], [16]. The steady state oscillations can be eliminated ideally. However, the null value of the slope of the PV array power versus the voltage curve rarely occurs due to the resolution of the digital implementation. Also the update rule of the controlling equation to reach the MPP is based on a fixed step size perturbation.

Although artificial intelligence algorithms (i.e., fuzzy logic control [17], neural networks [18], and genetic algorithms [19]), provide good alternatives to MPPT control as a non-linear control, the versatility of these methods is limited and the hardware implementation is very complex.

In fact, variable step size maximum power point trackers

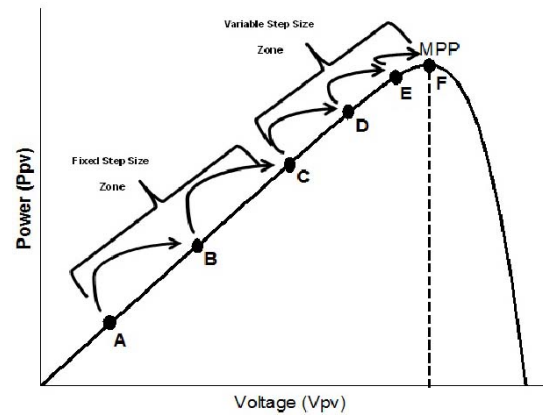


Fig. 3. Variable step size MPPT operation.

have been proposed for some techniques like the perturb and observe (P&O) method, the hill climbing method, and the incremental conductance (INC) method [12], [16], [20], [21], and [22]. The main idea in these algorithms is that the controller should satisfactorily address the tradeoff between the dynamics and the steady state oscillations as shown in Fig. 3. Almost all of these methods depend mainly on measuring the PV array output voltage and current. In the variable step size INC method, the updating rule for the step size depends on the derivative of the PV output power to the PV output voltage ( $\partial P/\partial V$ ), which is considered as a suitable parameter for determining the variable step size [16]. However, measuring the array power ( $P_{PV}$ ) and voltage ( $V_{PV}$ ) requires two sensors; one for measuring the current ( $I_{PV}$ ) and the other for measuring the voltage ( $V_{PV}$ ). Thus the experimental setup is more complicated and expensive.

This paper is organized as follows: the methodology for a stand-alone single current sensor based on a DC-DC boost converter is explained in section II. The proposed methods for a variable step size using a single current sensor are introduced in section III. A straight forward approach for designing the appropriate scaling factors is provided in section IV. Digital simulations and experimental results are presented in section V. Finally, a summary of the main results in this paper is provided in the conclusion.

## II. STAND-ALONE SINGLE CURRENT SENSOR MPPT

Different algorithms using only one variable measurement applied to a maximum power point tracker were proposed in [23], and [24]. Basically, the main idea behind this type of maximum power point tracking can be summarized as follow: when the output voltage of a DC-DC converter is regulated at a certain level, as in the case of battery storage systems or grid connected systems, the term of the PV array power will be reduced to a certain relationship between the PV array current and the converter duty cycle ( $D$ ).

For the stand-alone battery charging PV system equipped with a DC-DC boost converter shown in Fig. 4, the PV array power can be calculated as:

$$V_{bat} = \frac{1}{1-D} V_{PV} \quad (1)$$

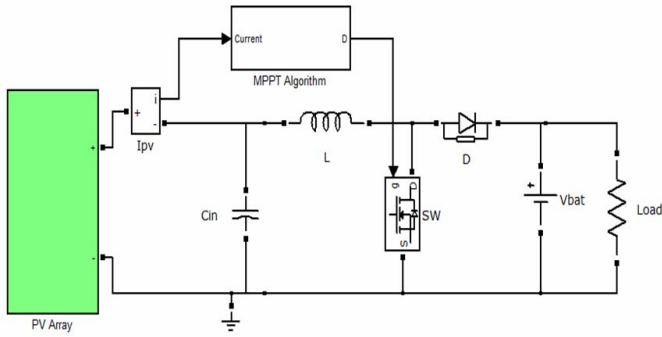


Fig. 4. Stand-alone single current sensor MPPT PV system equipped with DC-DC Boost converter.

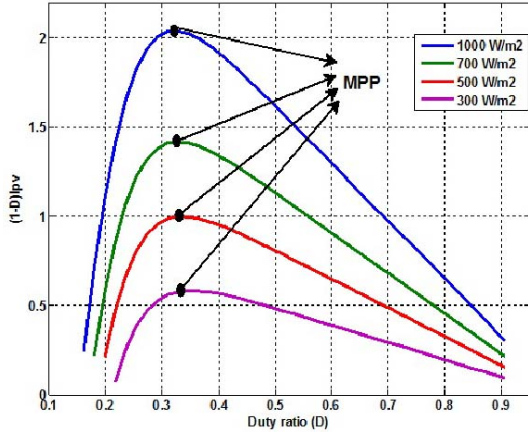


Fig. 5. Characteristic of the single current sensor MPPT with DC-DC boost converter at constant temperature 25°C.

$$\begin{aligned} P_{PV} &= V_{PV} I_{PV} \\ &= V_{bat} (1-D) I_{PV} \end{aligned} \quad (2)$$

where  $V_{PV}$ ,  $I_{PV}$ ,  $P_{PV}$ ,  $V_{bat}$ ,  $D$  correspond to the PV array voltage, the array current, the array power, the battery voltage (assumed to be constant), and the converter duty ratio, respectively.

The characteristic of  $[(1-D)I_{PV}]$  versus the converter duty ratio with different irradiation levels and different temperatures are shown in Fig. 5 and Fig. 6, respectively.

It can be concluded from Fig. 5 that the converter duty ratio, which corresponds to the maximum power point, can be considered motionless at different irradiation levels. This means that a battery storage PV system is more efficient in rapidly changing irradiation levels. However, from Fig. 6 it is obvious that the converter duty ratio, which corresponds to the maximum power point, varies significantly with different temperature conditions.

The tracking strategy for extracting the maximum power with single current sensor MPPT depends mainly on the hill climbing method [23], [27], [28] which applies a small perturbation and observe the resulting variation in the PV array power  $[(1-D)I_{PV}]$ . If the array power increases the following perturbation will be in the same direction as the last one. Otherwise the direction will be reversed. Therefore, as a consequence of the fixed step perturbation, the steady-state response will ensure steady-state oscillations around the MPP. The amplitude of these oscillations is directly proportional to the perturbation size ( $\Delta D$ ).

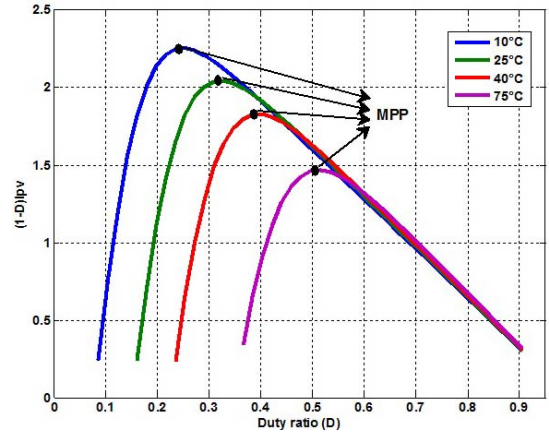


Fig. 6. Characteristic of the single current sensor MPPT with DC-DC boost converter at constant irradiation 1000 W/m<sup>2</sup>.

### III. PROPOSED VARIABLE STEP-SIZE MPPT

As discussed previously, the main idea to drive variable step size MPPT is to find a certain measure ( $Q$ ). This measure addresses the trade-off between the transient and the steady state performance. In another way, this measure ( $Q$ ) smoothly varies with the controlling variable ( $D$ ) to reach its minimum value at the MPP. Thus the updating variable step size equation has the form:

$$D(k+1) = D(k) + M * |Q| \quad (3)$$

where  $D(k+1)$ ,  $D(k)$ ,  $M$  correspond to the converter duty ratio at the instant  $(k+1)$ , the converter duty ratio at the instant  $(k)$ , and the scaling factor. In the following two methods are proposed for driving the variable step size based on (3).

#### A. Method 1

From Fig. 5 and Fig. 6 it is clear that the MPP occurs at the maximum value of  $[(1-D)I_{PV}]$  with respect to the converter duty cycle ( $D$ ). So the derivative of this quantity with respect to ( $D$ ) is considered to be a convenient measure to drive variable step size MPPT. Thus the updating equation is:

$$D(k+1) = D(k) + M_1 * \left| \frac{\partial G^*}{\partial D} \right| \quad (4)$$

where  $M_1$  and  $G^*$  correspond to the scaling factor and the value of  $[(1-D)I_{PV}]$ , respectively. Equation (4) can be rewritten in the digital form as:

$$D(k+1) = D(k) + M_1 * \left| \frac{G^*(k) - G^*(k-1)}{D(k) - D(k-1)} \right| \quad (5)$$

Although the idea of designing a variable step size using (5) is very simple, a certain shortcoming may be encountered. By inspecting (5), it is seen that the updating rule of the duty cycle depends on the absolute value of the difference between two successive instants of  $G^*$  divided by the difference between two successive instants of the converter duty cycle. The smoothness of this division requires a high sampling frequency and a high resolution analogue to digital converter. The required sampling frequency was optimized in [25]. Therefore, the vanishing value of this division rarely occurs and as a consequent the dynamic response of this method might have some steady state oscillation near the MPP.

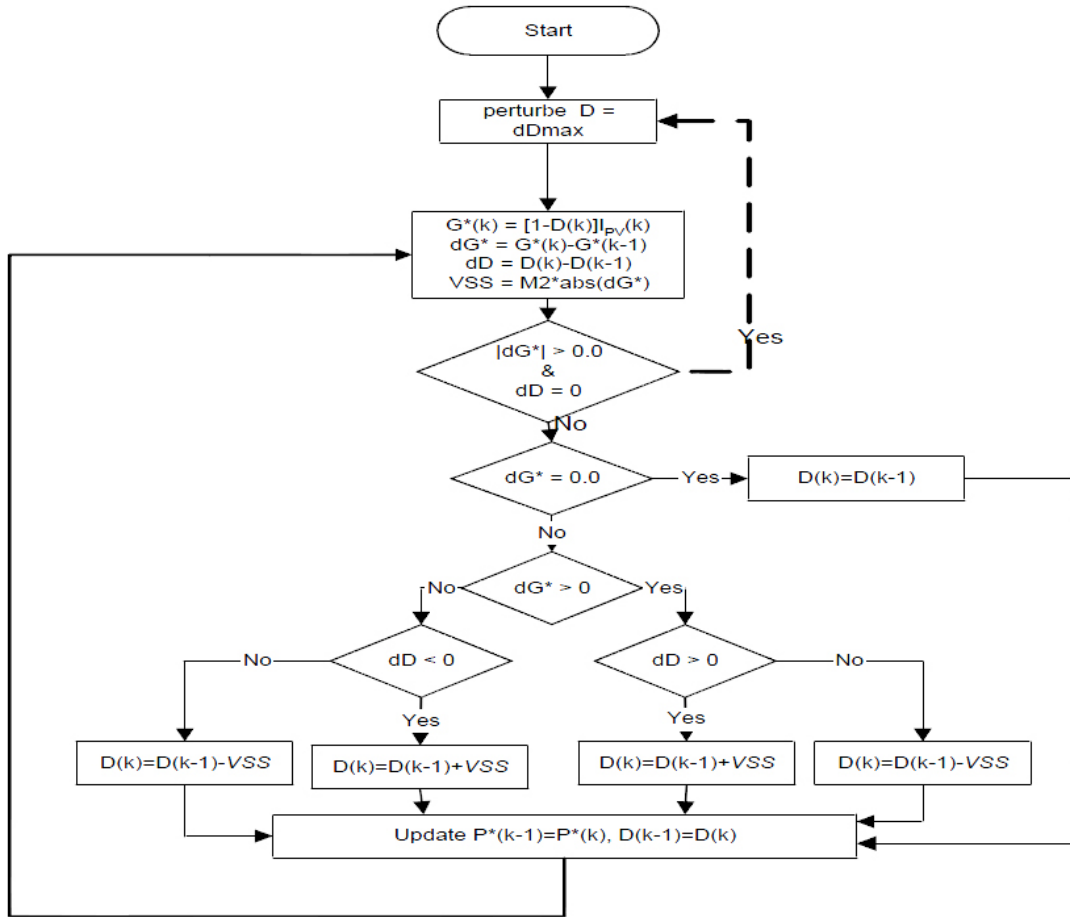


Fig. 7. Flowchart of the proposed variable step size MPPT using single current sensor (VSS represents variable step size).

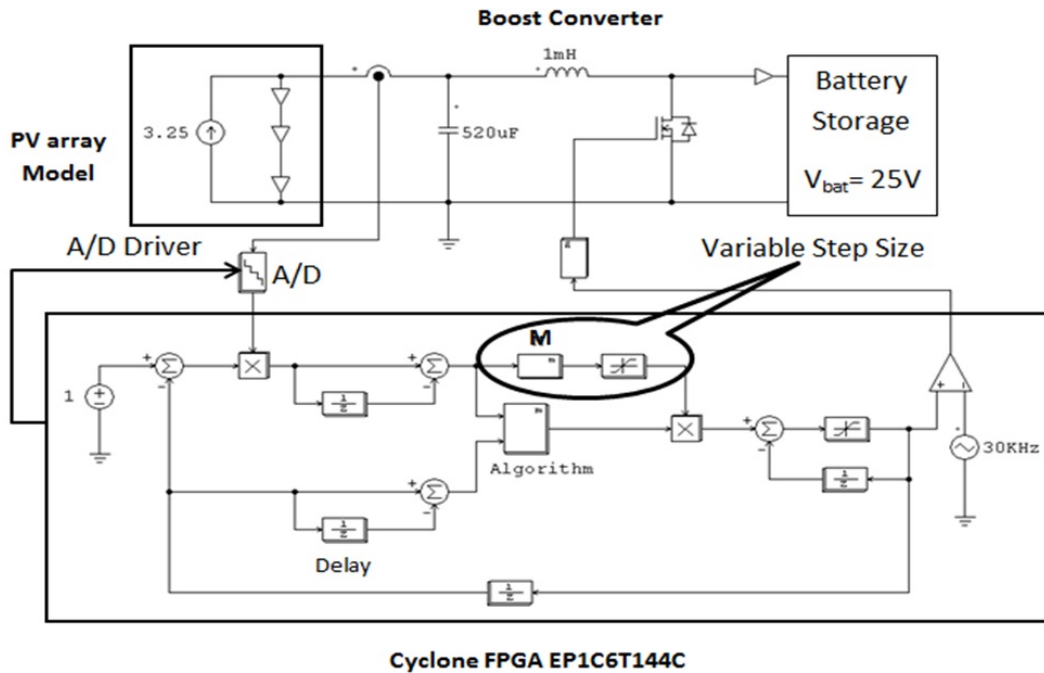


Fig. 8. Illustrative diagram of the hardware configuration equipped with a schematic diagram Of the proposed variable step size MPPT.



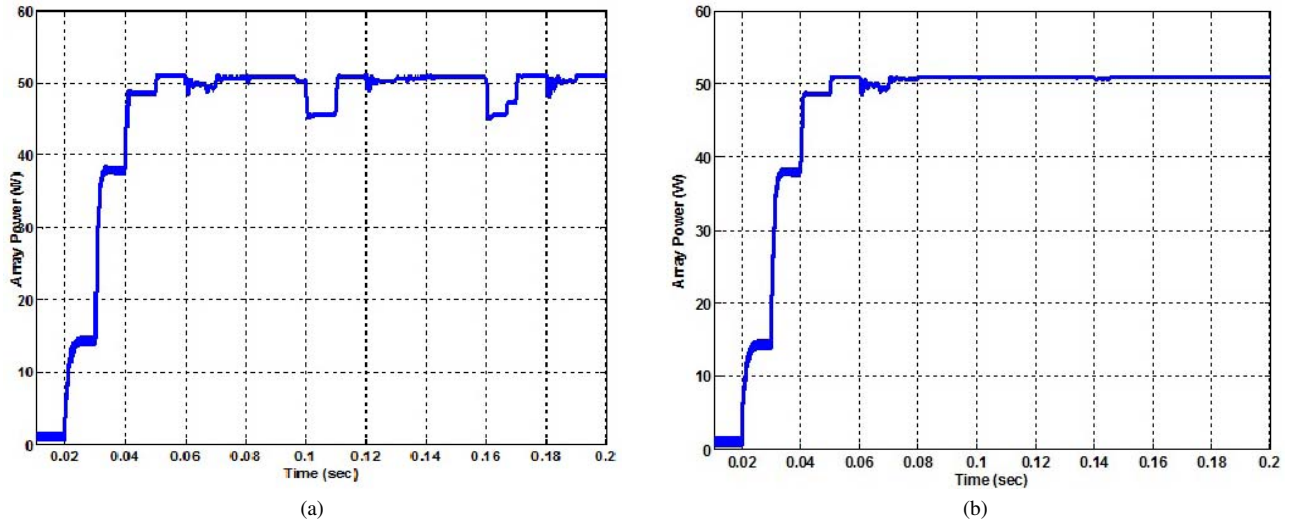


Fig. 9. Variable step size MPPT dynamic response with a step change in the irradiation from 0 to 1000 W/m<sup>2</sup>. (a) Method 1 ( $M_1 = 0.025$ ), (b) Method 2 ( $M_2 = 0.5$ ).

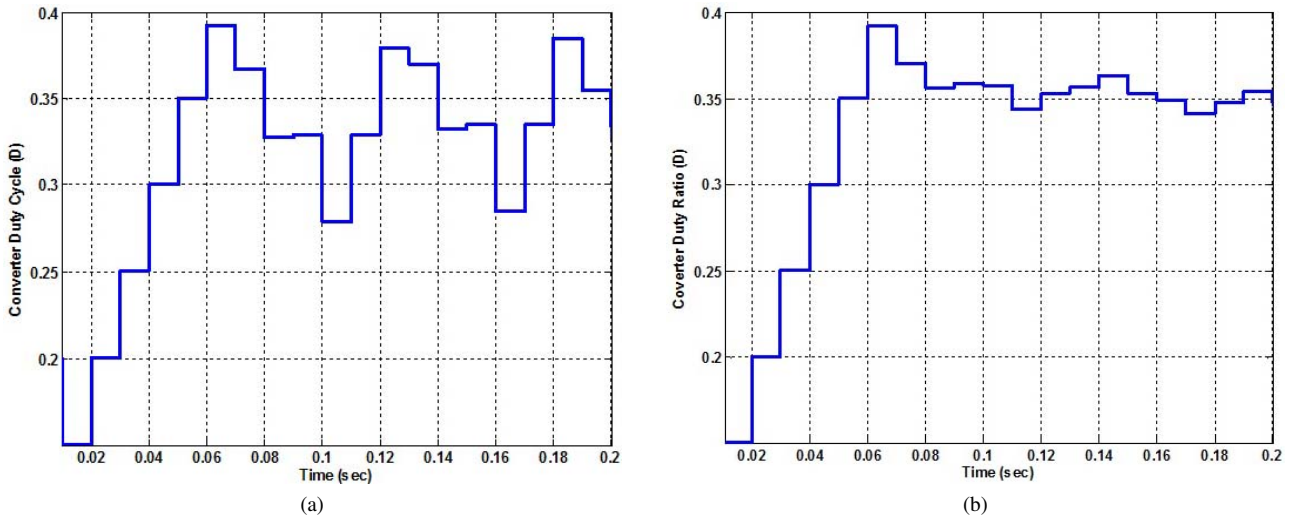


Fig. 10. Converter duty cycle ( $D$ ) at a step change in the irradiation from 0 to 1000 W/m<sup>2</sup>. (a) Method 1 ( $M_1 = 0.025$ ), (b) Method 2 ( $M_2 = 0.5$ ).

### B. Method 2

In order to overcome the above limitation, a certain modification has been proposed. After a through analysis of the characteristics of PV arrays, to develop a more robust variable step size MPPT, it is observed from Fig. 5 and Fig. 6 that the most appropriate alternative to replace the derivative of  $G^*$  versus  $D$  without highly complex computations and with more accuracy can be expressed as in (6).

$$D(k+1) = D(k) + M_2 * |\Delta G^*|. \quad (6)$$

The main idea behind this method depends on the variation of the difference between two successive instants of  $G^*$ .

By inspecting Fig. 5 and Fig. 6, the difference between two successive instants is large when the operating point is far from the MPP, while its value is tiny when the operating point is very close to the MPP. This is due to the flatness of the curve at the MPP. Moreover, equation (6) can be easily implemented

on an analogue or a digital circuit. An illustrative flowchart for the variable step size MPPT based on method 2 is shown in Fig. 7.

The main purpose of the dashed arrow is to reset the MPPT algorithm tracker from the steady state when there is any variation in the environmental conditions. Thus, the tracker begins with a fixed step size operation.

### IV. SCALING FACTOR DESIGN

Regarding the design of the scaling factor  $M$ , the scaling factor essentially determines the performance of the MPPT system. A low scaling factor ensures a slow transient response, while an outsized scaling factor can affect the variable step size and may result in operation with a fixed step size perturbation.

A simple method for designing the scaling factor  $M$  was proposed in [16]. The scaling factor can be designed for

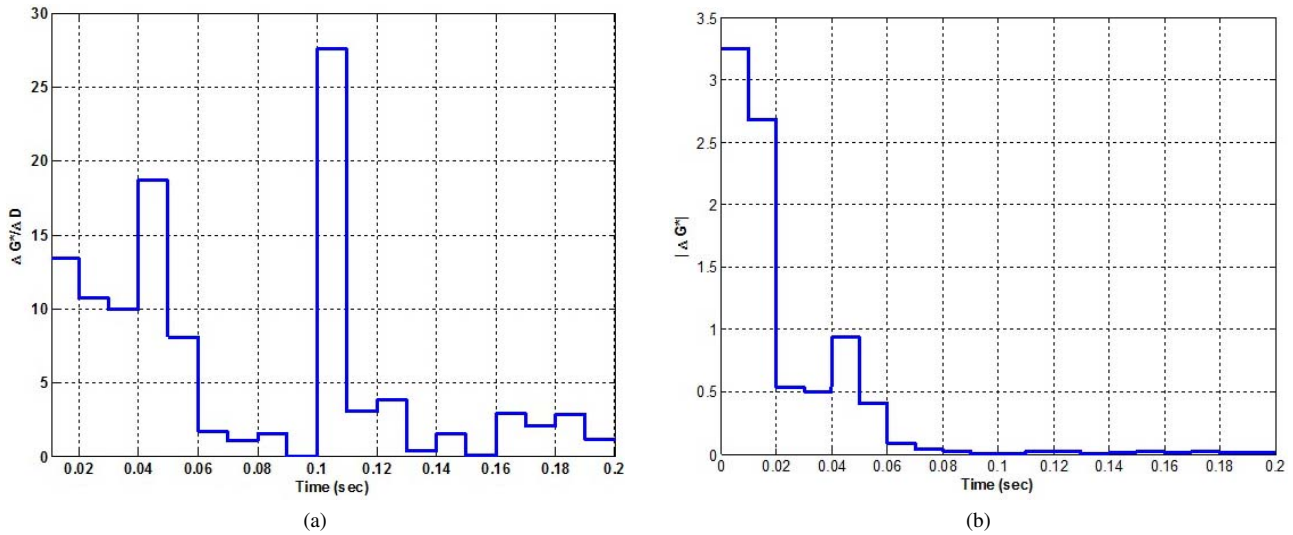


Fig. 11. Absolute value of the driving variable step size measure at a step change in the irradiation from 0 to  $1000 \text{ W/m}^2$ . (a) Method 1 ( $M_1 = 0.025$ ), (b) Method 2 ( $M_2 = 0.5$ ).

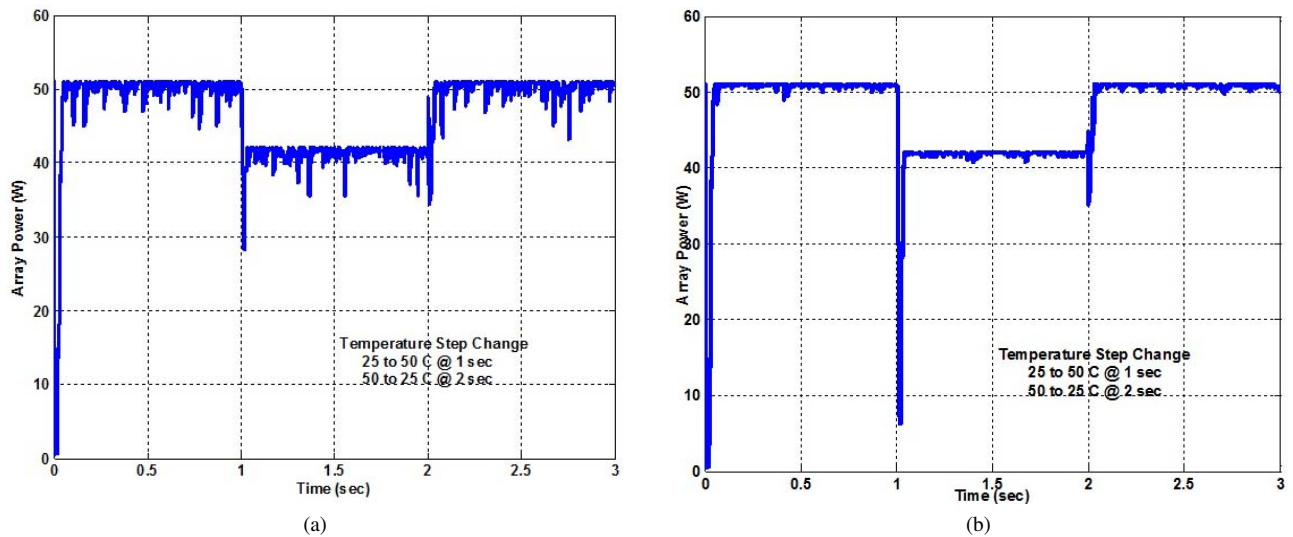


Fig. 12. Array power with the proposed variable step size MPPT due to Temperature Variation. (a) Method 1 ( $M_1 = 0.025$ ), (b) Method 2 ( $M_2 = 0.5$ ).

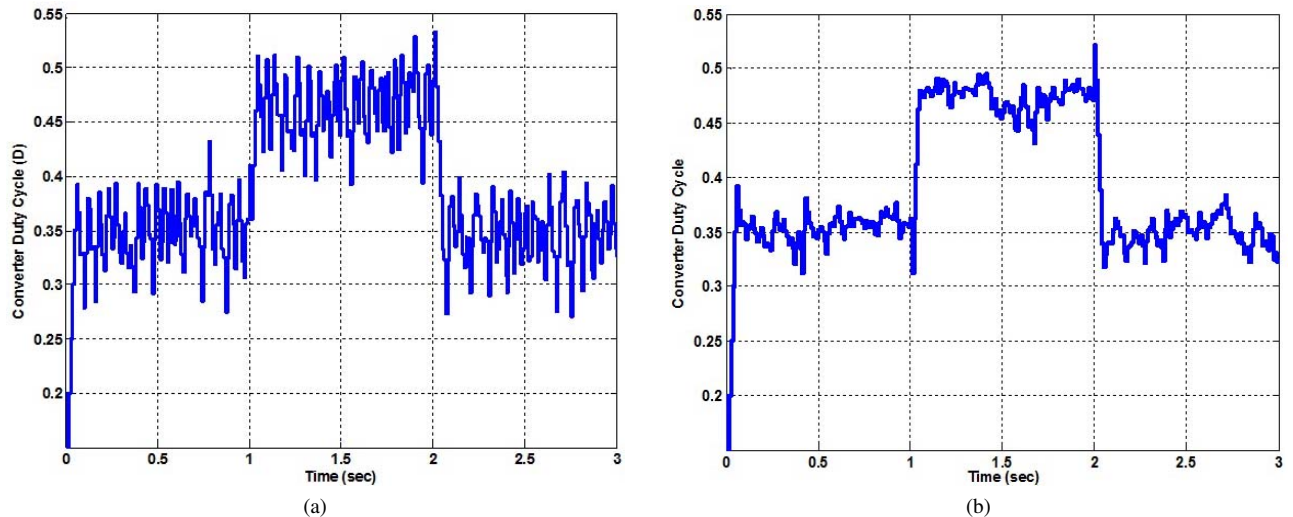


Fig. 13. Boost converter duty ratio ( $D$ ). (a) Method 1 ( $M_1 = 0.025$ ), (b) Method 2 ( $M_2 = 0.5$ ).

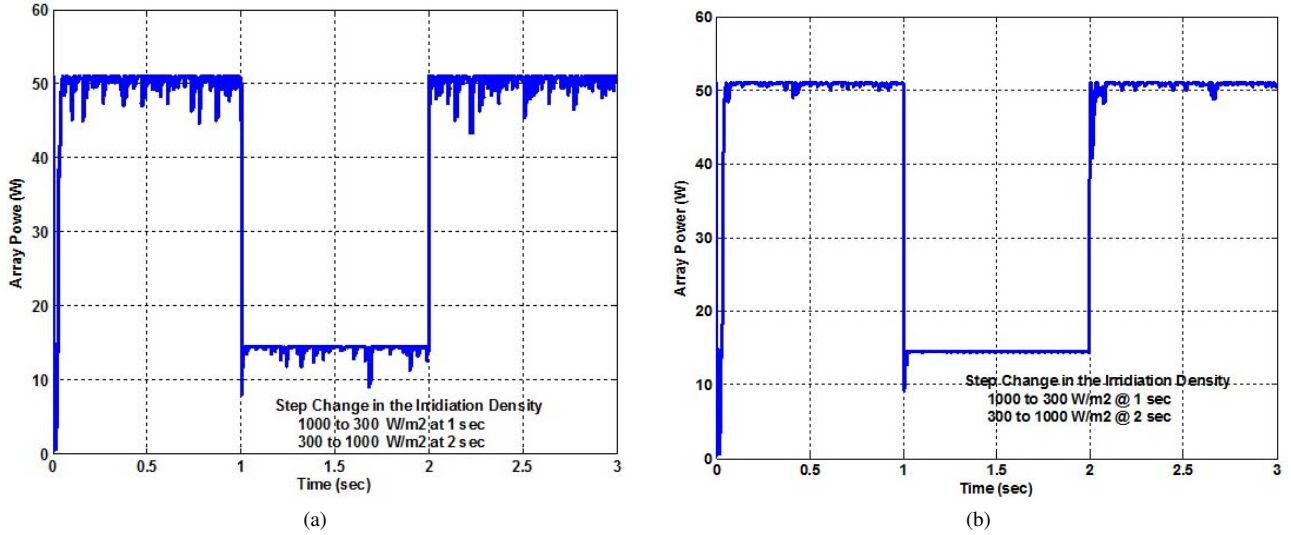


Fig. 14. Array power with the proposed variable step size. (a) Method 1 ( $M_1 = 0.025$ ), (b) Method 2 ( $M_2 = 0.5$ ).

method 1 as in (7):

$$0 < M_1 \leq \frac{\Delta D_{\max}}{\left| \frac{\Delta G^*}{\Delta D} \right|_{\text{Fixed step } \Delta D_{\max}}} \quad (7)$$

where  $\Delta D_{\max}$  is the maximum allowed fixed step size perturbation, which ensures a good transient response, and the numerator corresponds to the maximum steady state value of  $\Delta G^*/\Delta D$  with fixed step size operation ( $\Delta D_{\max}$ ).

Similarly, the scaling factor can be designed for method 2 as in (8):

$$0 < M_2 \leq \frac{\Delta D_{\max}}{\left| \Delta G^* \right|_{\text{Fixed step } \Delta D_{\max}}} \quad (8)$$

where the numerator corresponds to the maximum steady state value of  $\Delta G^*$  with fixed step size operation ( $\Delta D_{\max}$ ).

## V. DIGITAL SIMULATION RESULTS

To investigate the performance of variable-step size MPPT using the proposed methods, a PSIM model of a PV system was developed. An illustrative outline of the hardware configuration of the PV array and the proposed variable step size MPPT is shown in Fig. 8.

### A. PV Array Modelling

The PV array's electric characteristics are given in terms of the output current  $I_{PV}$  and voltage  $V_{PV}$  in (9) [26].

$$I_{PV} = I_H - I_o \left[ \exp \left( \frac{V_{PV} + I_{PV} R_s}{V_t} \right) - 1 \right] - \frac{V_{PV} + I_{PV} R_s}{R_{sh}} \quad (9)$$

where

$I_H = N_P I_{Ph}$  corresponds to the light-generated current of the solar array, where  $I_{Ph}$  is the cell light-generated current and  $N_P$  is the number of parallel modules.

$I_o = N_P I_{Os}$  corresponds to the reverse-saturation current of the solar array, where  $I_{Os}$  is the cell reverse current.

$V_t = N_s n K_B T / q$  is the thermal voltage, where  $N_s$  is the number of cells connected in series,  $K_B$  is the Boltzmann's constant,  $n$  is the ideality factor,  $T$  is the cell temperature, and  $q$  is the electron charge.

$R_s$  and  $R_{sh}$  represent the series and parallel parasitic resistance of a solar array, respectively.

The PV array current  $I_H$  can be calculated at different irradiance levels and array temperatures from (10):

$$I_H = (I_{H,n} + K_I \Delta T) \frac{G}{G_n} \quad (10)$$

where  $I_{H,n}$  is the light generated current under the nominal condition (usually  $25^\circ\text{C}$  and  $1000 \text{ W/m}^2$ ),  $\Delta T = T - T_n$ , ( $T$  and  $T_n$  being the actual and nominal temperature in Kelvin, respectively),  $G$  and  $G_n$  are the actual and nominal irradiance levels, respectively, and  $K_I$  corresponds to the array short circuit current temperature coefficient. The diode saturation current and its dependence on temperature may be expressed as in (11):

$$I_o = I_{o,n} \left( \frac{T_n}{T} \right)^3 \exp \left[ \frac{q E_g}{ak} \left( \frac{1}{T_n} - \frac{1}{T} \right) \right] \quad (11)$$

where  $E_g$  is the band-gap energy of the semiconductor ( $1.12 \text{ eV}$  for the polycrystalline Si at  $25^\circ\text{C}$ ) and  $I_{o,n}$  is the nominal saturation current which can be calculated by (12):

$$I_{o,n} = \frac{I_{sc,n}}{\exp(V_{OC,n}/a N_s V_{t,n}) - 1} \quad (12)$$

where  $I_{sc,n}$  corresponds to the nominal PV short circuit current,  $V_{OC,n}$  corresponds to the PV nominal open circuit voltage, and  $V_{t,n}$  corresponds the nominal cell thermal voltage. Therefore, with the aid of (9) through (12) a complete model of a PV array is constructed for simulation studies. The PV array parameters are shown in table I.

### B. Simulation Results

To investigate the performance of the proposed variable step size methods, a comparison has been made between designing

TABLE I  
PV ARRAY PARAMETERS (1000 W/M<sup>2</sup>, 25°C)

Open circuit voltage	21.2 V
Short circuit current	3.25 A
Nominal maximum power	51 W
Series resistance	0.35 Ω

the variable step size with method 1 and with method 2. The simulations are configured under exactly the same conditions. The sampling time for the MPPT algorithm is chosen to be 0.01 sec [26].

In order to design appropriate values for the scaling factors in the above methods, a simple procedure is proposed. First select the most appropriate desired fixed step size, which gives a fast transient response. Second with this fixed step size calculate by simulation the maximum desired value of the quantity, which drives the variable step size. Finally use (7) or (8) to define the scaling factors  $M_1$  and  $M_2$ , respectively.

By following the above procedure for designing the scaling factors  $M_1$  and  $M_2$ , it is determined that ( $0 < M_1 \leq 0.025$ ) for method 1, and that ( $0 < M_2 \leq 0.5$ ) for method 2. To ensure a good transient response the scaling factors  $M_1$  and  $M_2$  have been selected to be 0.025 and 0.5 for method 1 and method 2, respectively.

Fig. 9(a) and 9(b) show the dynamic performance of the variable step size MPPT designed by method 1 and method 2. It is obvious that both trackers track the MPP successfully without any diffraction. However both trackers have different performances in that, both trackers have the same transient response to reach the MPP of the array. This is as a result of selecting the maximum allowed value for the scaling factors. In the steady state both trackers have a somewhat different response. In Fig. 9(b), the tracker relaxed at the maximum power point (51 W) without any oscillation near it, while in the other case the tracker undergoes some oscillation near the MPP as shown in Fig. 9(a).

Fig. 10(a) and 10(b) try to give a reasonable understanding of the dynamic performance of these two methods. First, both of them have a fast transient response because they both operate with a fixed step size perturbation (0.05) for the first 8 samples ( $T_s = 0.01$  sec). Second, after they reach the MPP or a very near point to the MPP, a variable step size is adopted. In the first method the variable step size decreases and tries to increase at some instants due to an unsmooth variation of the derivative as shown in Fig. 11(a). However in the second method the variable step size decreases to lower value and tries to keep its lower value as shown in Fig. 11(b). As a result, the array power suffers from fluctuations in the second method.

To investigate the wider range performance of both trackers, the dynamic responses of the PV array power with a step change in the array temperature have been checked in Fig. 12(a) and Fig. 12(b). It is evident that the variable step size MPPT designed by the second method has a good transient and steady state response as shown in Fig. 13(b). However, the variable step size MPPT designed by method 1 suffers from a higher fluctuation near the MPP as can be seen from the converter duty cycle in Fig. 13(a).

Furthermore, the dynamic performance of both trackers has been examined with different irradiation densities as shown in

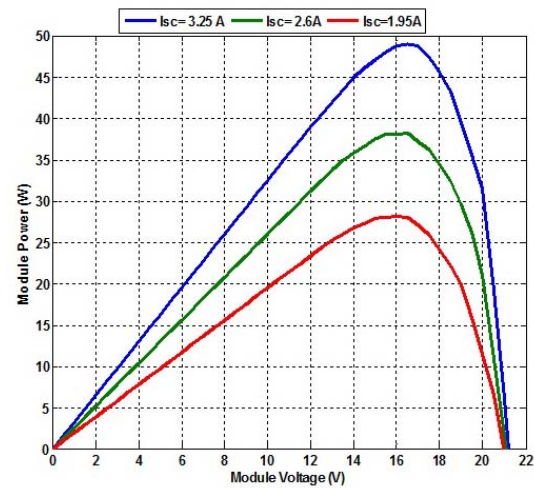


Fig. 15. P-V array characteristics of the experimental PV Array model.

Fig. 14(a) and 14(b).

It is clear from the above results that the proposed variable step size MPPT methods track successfully. However, the variable step size MPPT designed with method 2 has a better transient and steady state response than the variable step size MPPT designed with method 1.

### C. Experimental Results

A descriptive diagram of the hardware configuration and the MPPT algorithm is shown in Fig. 8. The power circuit consists of a PV module, a DC-DC Boost converter, and a constant voltage load (25 V). The PV array is experimentally constructed with a string of series diodes and a current source supply ( $V_{OC} = 21$  V,  $I_{SC} = 3.25$ ) as shown in Fig. 8. The P-V characteristics of this module are plotted at different short circuit currents as shown in Fig. 15. The short circuit currents 3.25A, 2.6A, and 1.95A represent the irradiation densities 1000, 800, and 600 W/m<sup>2</sup>, respectively. The control circuit was configured and implemented with the aid of a cyclone FPGA 66 MHz equipped with an 8 bit A/D converter, which was programmed with the MPPT control algorithm and the automatic tuning variable step size loop.

Fig. 15 shows the performance of the PV array in the experimental setup. Only the variable step size MPPT designed with method 2 has been implemented.

The dynamic response of the PV array power has been checked in different situations. Fig. 16(a) shows the dynamic response of the array power, the voltage, and the current when there is a step change in the array short circuit current (when  $I_{sc}$  is switched from 0 to 3.25 A) with fixed step size of ( $\Delta D = 0.05$ ). Fig. 16(b) shows the dynamic performance of the proposed variable step size MPPT designed with method 2. It is clear that the steady state oscillations are completely removed.

To demonstrate the importance of designing the scaling factor, Fig. 16(c) shows the dynamic performance of a PV array with a scaling factor greater than the one that was designed by (8). It obvious that the dynamic response becomes worse.



## VI. CONCLUSIONS

In this paper, two variable step size maximum power point trackers for stand-alone battery storage PV systems based on single variable measurement have been proposed. Both methods tune the variable step size MPPT based-on the relationship between the array current and the corresponding converter duty cycle ( $D$ ).

In the first method, the variable step size is derived from the derivative of  $[(1-D)I_{PV}]$  versus  $D$ . By examining this method through simulation, it has been found that it might suffer from steady state fluctuations due to the digital implementation and the sampling period.

In the second method, the variable step size was tuned from the difference between two successive samples of  $[(1-D)I_{PV}]$ . Through digital simulation and experimental verification, this method has demonstrated good transient and steady state performance.

The main ideas behind the second method can be generalized to any variable step size maximum power point tracker.

## REFERENCES

- [1] V. Salas, E. Olias, and A. Lázaro, "Review of the maximum power point tracking algorithms for stand-alone photovoltaic systems," *Solar Energy Materials and Solar Cells*, Vol. 90, pp. 1555-1578, Jul. 2006.
- [2] C. Rodriguez and G. Amarantunga, "Analytic solution to the photovoltaic maximum power point problem," *IEEE Trans. Circuits Syst.*, Vol. 54, No. 9, pp. 2054-2060, Sep. 2007.
- [3] H. Bae, J. Lee, S. Park, and B. Cho, "Large-signal stability analysis of solar array power system," *IEEE Trans. Aerosp. Electron. Syst.*, Vol. 44, No. 2, pp. 538-547, Apr. 2008.
- [4] W. Jiang and B. Fahimi, "Multi-port power electronic interface for renewable energy sources," in *Proc. APEC*, pp. 347-352, 2009.
- [5] T. Tafticht, K. Agbossou, M. L. Dombia, and A. Chériti, "An improved maximum power point tracking method for photovoltaic systems," *Renewable Energy*, Vol. 33, No. 7, pp. 1508-1516, Jul. 2008.
- [6] G. de Cesare, D. Caputo, and A. Nascetti, "Maximum power point tracker for portable photovoltaic systems with resistive-like load," *Solar Energy*, Vol. 80, No. 8, pp. 982-988, Aug. 2006.
- [7] V. Scarpa, S. Buso, and G. Spiazzi, "Low-complexity MPPT technique exploiting the PV module MPP locus characterization," *IEEE trans. Ind. Electron.*, Vol. 56, No. 5, pp.1513-1538, May 2009.
- [8] T. Esram, J. W. Kimball, P. T. Krein, P. L. Chapman, and P. Midya, "Dynamic maximum power point tracking of photovoltaic arrays using ripple correlation control," *IEEE trans. Ind. Electron.*, Vol. 21, No. 5, pp. 1282-1291, Sep. 2006.
- [9] J.-A. Jiang, T.-L. Huang, Y.-T. Hsiao, and C.-H. Chen, "Maximum power tracking for photovoltaic power systems," *Tamkang Journal of Science and Engineering*, Vol. 8, No. 2, pp. 147-153, 2005.
- [10] K. Itako and T. Mori, "A current sensor less MPPT control method for a stand-alone-type PV generation system," *Journal of Electrical Engineering in Japan*, Vol. 157, No. 2, pp. 65-71, Aug. 2006.
- [11] T. Esram and P. Chapman, "Comparison of photovoltaic array maximum power point tracking techniques," *IEEE trans. on Energy Conversion*, Vol. 22, No. 2, pp. 439-449, Jun. 2007.
- [12] L. Piegari and R. Rizzo, "Adaptive perturb and observe algorithm for photovoltaic maximum power point tracking," *IET Renewable. Power Gen.*, Vol. 4, No. 4, pp. 317-328, Jul. 2010.
- [13] N. Femia, D. Granozio, G. Petrone, and M. Vitelli, "Predictive & adaptive MPPT perturb and observe method," *IEEE trans. Aerosp. Electron. Syst.*, Vol. 43, No. 3, pp. 934-950, Jul. 2007.
- [14] N. Khaehintung, T. Wiangtong, and P. Sirisuk, "FPGA implementation of MPPT using variable step-size P&O algorithm for PV applications," *In Proc. ISCIT*, pp. 212-215, 2006.
- [15] G.-J. Yu, J.-Y. Choi, and G.-S. Kim, "A novel two-mode MPPT control algorithm based on comparative study of existing algorithms," *Solar Energy*, Vol. 76, No. 4, pp. 455-463, Apr. 2004.
- [16] F. Liu, S. Duan, F. Liu, B. Liu, and Y. Kang, "A variable step size INC MPPT method for PV systems," *IEEE trans. on Industrial. Electronics*, Vol. 55, No. 7, pp. 2622-2628, Jul. 2008.

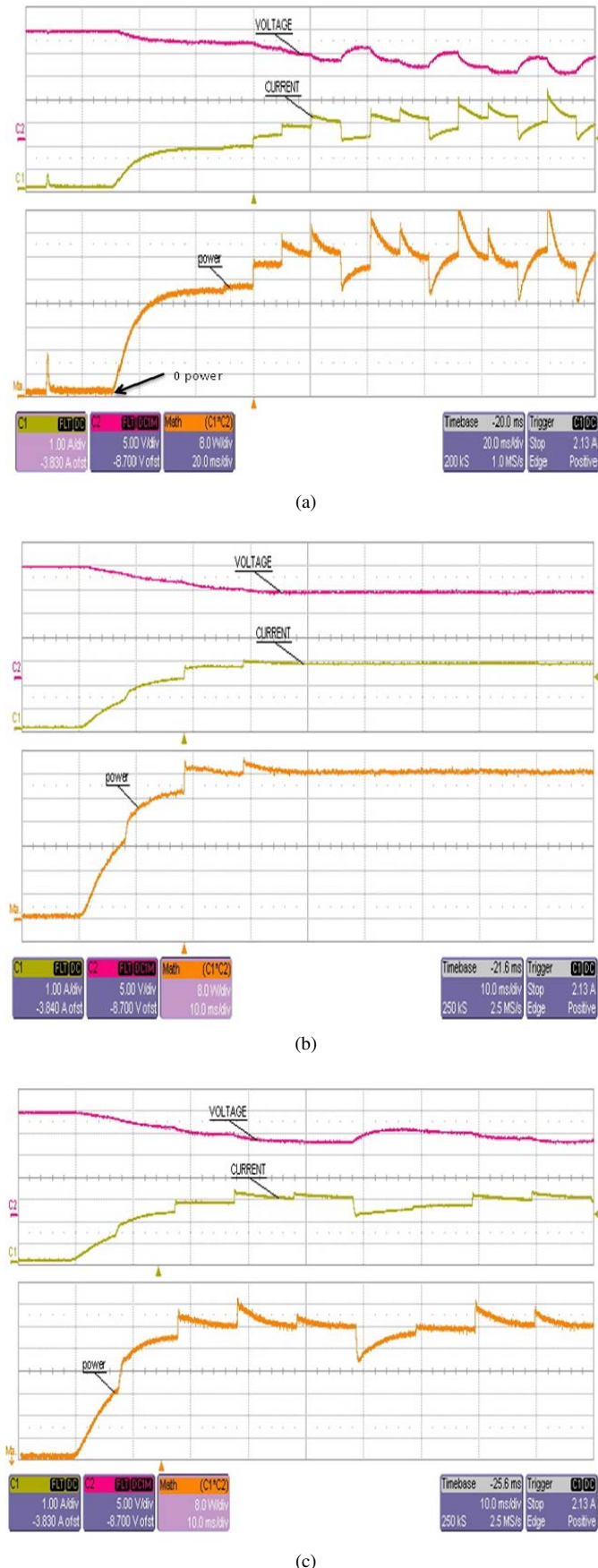


Fig. 16. 3.25A step change in the  $I_{sc}$  (A) with method 2. (a) Fixed step (0.05). (b)  $M_2 = 0.5$  (c)  $M_2 > 0.5$ .

- [17] S. Lalouni, D. Rekioua, T. Rekioua, and E. Matagne, "Fuzzy logic control of stand-alone photovoltaic system with battery storage," *Journal of Power Sources*, Vol. 193, pp. 899-907, Sep. 2009.
- [18] K.-H. Chao and C.-J. Li, "An intelligent maximum power point tracking method based on extension theory for PV systems," *Journal of Expert Systems with Applications*, Vol. 37, pp. 1050-1055, Mar. 2010.
- [19] C. Larbes, S. Cheikh, T. Obeidi, and A. Zerguerras, "Genetic algorithms optimized fuzzy logic control for the maximum power point tracking in photovoltaic system," *Renewable Energy*, Vol. 34, No. 10, pp. 2093-2100, Oct. 2009.
- [20] N. S. D'Souza, L. A. Lopes, and X. Liu, "Comparative study of variable step size perturbation and observation maximum power point trackers for PV systems," *Electric Power System Research*, Vol. 80, No. 3, pp. 296-305, Mar. 2010.
- [21] W. Xiao and W. G. Dunford, "A modified adaptive hill climbing MPPT method for photovoltaic power systems," in *Proc. PESC*, pp. 1957-1963, 2004.
- [22] A. Pandey, N. Dasgupta, and A. K. Mukerjee, "Design issues in implementing MPPT for improved tracking and dynamic performance," in *Proc. IECON*, pp. 4387-4391, 2006.
- [23] V. Salas, E. Olias, A. Lazaro, and A. Barrado, "New algorithm using only one variable measurement applied to a maximum power point tracker," *Solar Energy Materials and Solar Cells*, Vol. 87, pp. 675-684, May 2005.
- [24] V. Salas, E. Olias, A. Lazaro, and A. Barrado, "Evaluation of a new maximum power point tracker applied to the photovoltaic stand-alone systems," *Solar Energy Materials and Solar Cells*, Vol. 87, pp. 807-815, May 2005.
- [25] N. Femia, G. Petrone, and M. Vitelli, "Optimization of perturb and observe maximum power point tracking method," *IEEE Trans. Ind. Electron.*, Vol. 20, No. 4, pp. 963-973, Jul. 2005.
- [26] M. Gradella, J. Rafael, and E. Ruppert, "Comprehensive approach to modeling and simulation of photovoltaic arrays," *IEEE Trans. Power Electron.*, Vol. 24, No. 5, May 2009.
- [27] E. M. Ahmed and M. Shoyama, "Highly Efficient Variable Step Size Maximum Power Point Tracker for PV Systems," in *Proc. ISEEE*, pp. 112-117, 2010.
- [28] E. M. Ahmed and M. Shoyama, "Modified Adaptive Variable Step Size MPPT Based-on Single Current Sensor," in *Proc. TENCON*, pp. 1235-1240, 2010.



**Emad M. Ahmed** received his B.Sc. and M.Sc. in Electrical Engineering from South Valley University, Aswan, Egypt, in 2001 and 2006, respectively. He is currently working toward his Ph.D. in the Department of Electrical Engineering, Graduate School of Information Science and Electrical Engineering, Kyushu University, Fukuoka, Japan. Since 2002, he has been associated with the Department of Electrical Engineering, Faculty of Engineering, South Valley University, first as a Teaching Assistant and since 2006, as a Lecturer Assistant. His current research interests include power electronics, especially in renewable energy applications, artificial intelligence, and digital control. He is a student member of IEEJ, IEEE Power Electronics Society (PELS), and IEEE Industrial Electronics Society (IES).



**Masahito Shoyama** received his B.S. in Electrical Engineering and his D.Eng. from Kyushu University, Fukuoka, Japan, in 1981 and 1986, respectively. He joined the Department of Electronics, Kyushu University as a Research Associate in 1986, and became a Professor in 2010. Since 1996, he has been with the Department of Electrical and Electronic Systems Engineering, Graduate School of Information Science and Electrical Engineering, Kyushu University. He has been active in the field of power electronics, especially in the areas of high-frequency switching power supplies, power factor correction, piezoelectric power converters, and electromagnetic compatibility (EMC). Dr. Shoyama is a member of IEEE, IEICE, IEEJ and SICE.